Eur. J. Stat. 4 (2024) 2
doi: 10.28924/ada/stat.4.2

Improved Monitoring of Early-Warning Signs of an AMOC Collapse

Erhard Reschenhofer

Retired from University of Vienna, Austria

Correspondence: erhard.reschenhofer@univie.ac.at

ABSTRACT. This paper reviews a recent study predicting that the Atlantic Meridional Overturning Current circulation may collapse in the middle of this century and concludes that there are too many uncertainties to allow a reliable prediction. Even if the model used in that study is fairly adequate, its predictions depend heavily on the quality of the involved approximations, the choice of the circulation proxy, the method of trend estimation, the size of the rolling window used for the estimation of the second moments, the determination of the start time of ramping, etc. Forced to set lower targets, the focus is consequently shifted to the improved detection of early-warning signs like an increase in variance and autocorrelation. Two new estimation procedures are introduced. The first concerns the estimation of the trend and includes a new criterion for comparing the quality of different estimates. The second is a procedure for detecting changes in the first-order autocorrelation without any delay caused by an estimation window. The results obtained with these methods suggest that the autocorrelation increases erratically rather than steadily which would make forecasting based on extrapolation impossible.

1. INTRODUCTION

The Atlantic Meridional Overturning Current (AMOC), of which the Gulf Stream is a part, is caused by differences in temperature and salinity in different regions. Latif et al. (2004) found a close relationship between multidecadal variations in the strength of this circulation and Atlantic sea-surface temperature (SST) and proposed to use this relationship for the reconstruction of past changes and the monitoring of future changes in the strength of the AMOC using SST

Received: 21 Aug 2023.

Key words and phrases. Global warming; tipping point; AMOC; early-warning signs; variance; autocorrelation.

observations only. Rahmstorf et al. (2015) identified the geographic region in the North Atlantic that is most sensitive to a reduction in the AMOC and referred to it as "'subpolar gyre". Assuming that differences in surface temperature evolution between the subpolar gyre and the whole Northern Hemisphere are largely due to changes in the AMOC, they defined an AMOC proxy by subtracting the Northern Hemisphere mean surface temperature from that of the subpolar gyre.

Given the hypothesis that a slowdown of the AMOC leads to a region of relative cooling near the subpolar gyre and a region of above-average warming in the vicinity of the Gulf Stream, Caesar et al. (2018) tested whether the temperatures in these regions can be used to reconstruct changes in the AMOC. It turned out that the warm patch is unsuitable for that purpose because of its high variability. Thus, they decided to base their AMOC proxy only on the cold patch. It is defined as the mean temperature of the subpolar gyre minus the global mean SST. Jackson and Wood (2020) compared many different proxies including those proposed by Rahmsdorf et al. (2015) and Caesar et al. (2018) and concluded (not unexpectedly) that it depends on the question being asked which proxy is the best. They also conceded that their results may depend on the particular climate model they have used to conduct their analysis.

According to some climate models, the AMOC has two different stable circulation modes. The transition from the present strong mode to the weak mode can, for example, be triggered by reducing salinity via enhanced meltwater inflow into the North Atlantic. Boers (2021) investigated several SST-based and salinity-based AMOC proxies. His findings suggest that the AMOC could be close to a critical transition to its weak circulation mode. Using a similar model as Boers (2021), Ditlevsen & Ditlevsen (2023) went one step further and tried to determine when this critical transition will happen. In their widely noticed study, they predicted with high confidence (95%) and under the usual caveats that the AMOC could collapse as early as 2025 and not later than 2095. In contrast, the experts of the UN's Intergovernmental Panel on Climate Change believe that the AMOC will only weaken but not collapse in the 21st century (IPCC, 2019).

In view of this discrepancy, we will take a closer look at the former study in Section 2 with a focus on the statistical methodology, or more precisely on the

moment-based estimator of the tipping time. We will not investigate the second estimator used in that study, firstly because it is less robust as it depends more heavily on the correct specification of the underlying model and secondly because its predictions are very similar to those of the first estimator. Section 2 shortly describes the model, sheds some light on the arbitrariness in the specification of the tuning parameters, and tries to replicate some of the results.

The moment-based estimator of the tipping time uses the variance and the first-order autocorrelation as predictors of a forthcoming structural change in the dynamics. An increase in the variance and an increase in the autocorrelation are early-warning signs. Since the variance measures the deviation from the mean and the autocorrelation measures the relationship between successive deviations, a false alarm will be the inevitable consequence if the increase in the mean due to global warming is not properly taken care of. The standard approach to estimate a time-varying mean is to calculate moving averages. In Section 3, it is argued that this method is not ideal when forecasting is the objective. Global nonparametric smoothing techniques are preferable because they allow the earlier detection of changes in variance and autocovariance. The autocorrelation is a different story. Unfortunately, the only available method for the detection of a change in the first-order autocorrelation $\rho(1)$ without any delay caused by an estimation window (Reschenhofer, 2017a) relies on the assumption that $\rho(1)$ is small. But since $\rho(1)$ increases toward 1 when the system edges closer to a structural change, an adjustment is necessary. Two variants are discussed. Section 3 also introduces a new method to compare the quality of different trend estimates. Section 4 concludes.

2. ESTIMATING THE TIME OF THE AMOC COLLAPSE

2.1 THE MODEL

Suppose that at time t_0, the control parameter $\lambda < 0$ of the stochastic differential equation

$$dX_t = F'(X_t)dt + \sigma B_t,\ F'(x) = f(x) - \lambda = -A(X-m)^2 - \lambda,\ A > 0, \qquad (1)$$

which might to some extent describe the dynamics of an AMOC proxy $X(t)$, begins to grow linearly and reaches the value 0 at time t_c, where the dynamical system transitions from the present state with a local minimum of the function $F(x)$ at $x_1 = m + \sqrt{-\lambda/A}$ and a local maximum at $x_2 = m - \sqrt{-\lambda/A}$ to a new state. Using the first-order Taylor approximation of $F'(x)$ in the neighborhood of x_1, we obtain

$$\begin{aligned} F'(x) &\approx F'(x_1) + F''(x_1)(x - x_1) = 0 + f'(x_1)(x - x_1) = -2A(x - m)(x - x_1) \\ &= -2A\left(x - x_1 + \sqrt{-\lambda/A}\right)(x - x_1) = -2A\sqrt{-\lambda/A}\ (x - x_1)\ -2A(x - x_1)^2 \\ &\approx -2A\sqrt{-\lambda/A}\,(x - x_1) = -2\sqrt{-\lambda A}\,(x - x_1) = -\alpha(x - x_1). \end{aligned} \tag{2}$$

Within a short time interval, λ is approximately constant and the dynamics of $X(t)$ may therefore in a neighborhood of x_1 be approximated by the Ornstein–Uhlenbeck process

$$dX_t = -\alpha(X_t - x_1)dt + \sigma B_t, \tag{3}$$

which is driven by the Brownian motion B_t. The parameters of this process can be obtained locally from estimates of its moments. The mean and the autocovariances are given by $\mu = x_1$ and

$$cov(X_s, X_t) = \frac{\sigma^2}{2\alpha} exp(-\alpha|t - s|), \tag{4}$$

respectively. Given a sample $X_1, \ldots, X_T$ of monthly observations, we can estimate $\mu = x_1$,

$$\gamma(0) = var(X_t) = \frac{\sigma^2}{2\alpha}, \tag{5}$$

$$\rho(1) = cor\left(X_t, X_{t+1/12}\right) = exp(-\alpha/12), \tag{6}$$

α, σ^2, and $\tau = A\lambda$ by the sample mean $\bar{X}$, the sample variance $\hat{\gamma}(0)$, the sample autocorrelation $\hat{\rho}(1)$, $\hat{\alpha} = -12\, log(\hat{\rho}(1))$, $\hat{\sigma}^2 = 2\hat{\alpha}\ \hat{\gamma}(0)$, and $\hat{\tau} = -\hat{\alpha}^2/4$, respectively.

Now if we really think that our dynamic model is suitable, all of our approximations are harmless, and the assumption of a linearly changing control parameter λ is correct, we could boldly try to estimate the time of the collapse of the extremely complex AMOC system just by estimating the squared log first-order autocorrelation of some AMOC proxy locally and linearly extrapolating the

local estimates until we reach the critical limit of zero. The estimated time of collapse would, of course, still depend heavily on the chosen estimation method.

2.2 THE ESTIMATION

Given observations $X_1,\ldots,X_n$ of an AMOC proxy, Ditlevsen & Ditlevsen (2023) used a rolling window of size $T = 1 + 55 * 12$ to obtain a sequence $\hat{\gamma}_1(0),\ldots,\hat{\gamma}_{n-T+1}(0)$ of sample variances as well as a sequence $\hat{\rho}_1(1),\ldots,\hat{\rho}_{n-T+1}(1)$ of sample autocorrelations and fitted a broken linear trend with a zero slope until $t_0 = 1924$ (December 1923) to the sequence $\hat{\tau}_1,\ldots,\hat{\tau}_{n-T+1}$, where

$$\hat{\tau}_t = -36\, log^2(\hat{\rho}_t(1)), k = 1,\ldots,n-T+1. \tag{7}$$

For the estimation of the transition time t_c, they extrapolated the nonzero slope in the second regime (starting January 1924) and found a crossing of the *x*-axis in the year 2057. However, when I tried to replicate their results (with the free statistical software R; see R Core Team, 2022), I found the crossing already in 2026 although I used the same data (obtained by the authors from the Hadley Centre Sea Ice and Sea Surface Temperature data set HadISST, see 26) which were kindly provided by Ditlevsen & Ditlevsen (2023) online in a repository. My Figure 1 shows the AMOC proxy in (a), the sample variances in (b), the sample autocovariances in (c), the estimates of α in (d), the estimates of σ^2 in (e), and the estimates of $-\tau = -A\lambda$ in (f). All figures except the last one look exactly like their counterparts in Figure 5 of Ditlevsen & Ditlevsen (2023). Unfortunately, the last one is just the one needed to determine the transition time t_c. According to the labels in their Figure 5, the (estimated) quantity $A\lambda$ is calculated as

$$A\lambda = \left(\frac{\sigma^2}{4\gamma(0)}\right)^2 = \left(\frac{2\alpha\gamma(0)}{4\gamma(0)}\right)^2 = \frac{\alpha^2}{4} \tag{8}$$

and therefore differs from (2) just in the sign. However, this possible sign error has no effect on the estimate of t_c. It makes no difference whether a positive line decreases toward zero or its negative counterpart increases toward zero. Nevertheless, for reasons of comparability, the quantities $-\hat{\tau}_k$ are shown in my Figure 1.f. An obvious problem of their Figure 5 is that $\alpha^2/4$ shown in 5.f is inconsistent with α shown in 5.d. But quite apart from these minor problems, predictions of this type are in general extremely unreliable. There are just too

many uncertain assumptions and approximations, too much data snooping (e.g., for the determination of the time of the structural break and the size of the rolling window) etc.

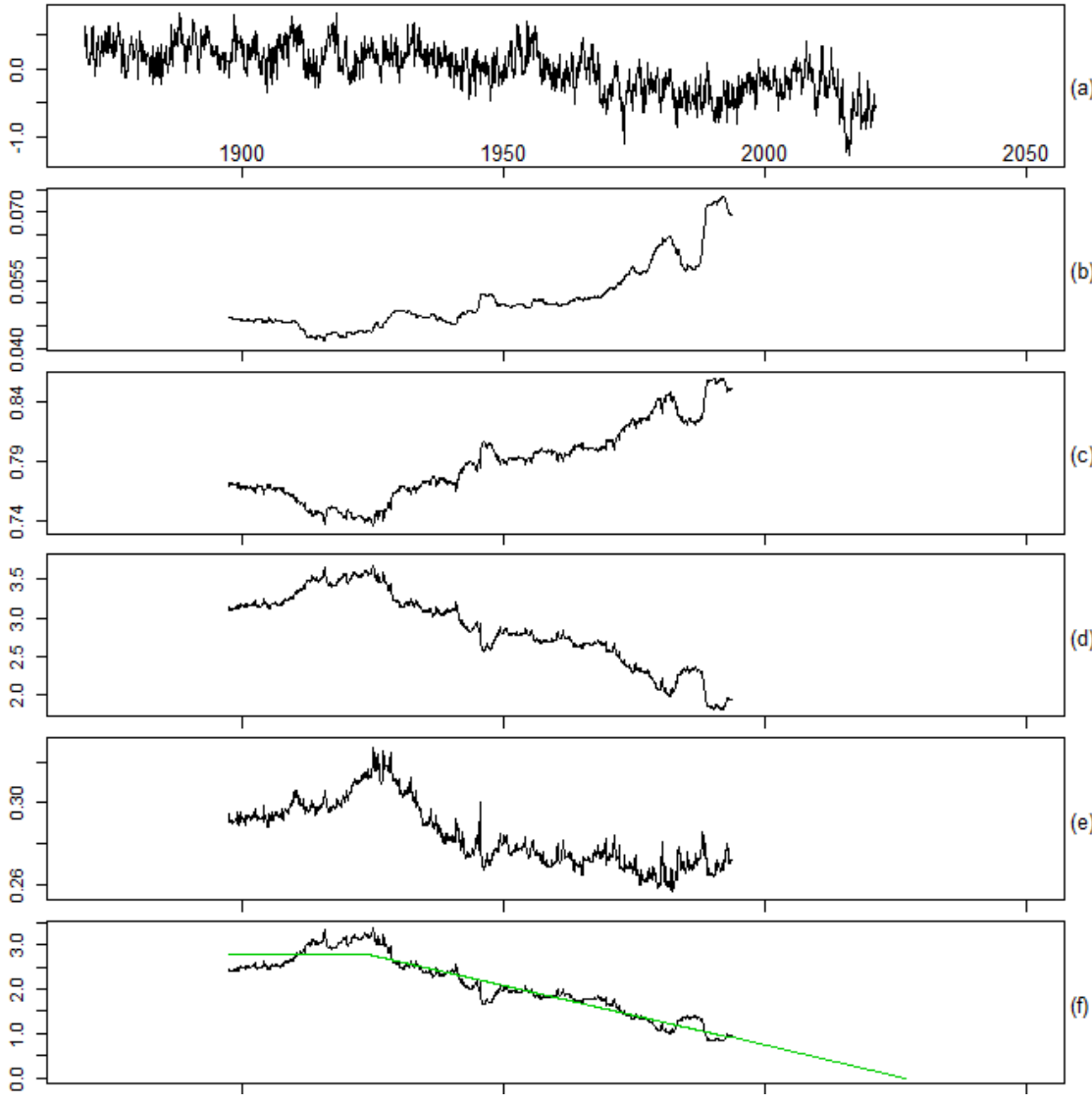

Figure 1: (a) AMOC proxy defined as the mean temperature of the subpolar gyre minus two times the global mean SST
(b)-(f) Rolling-window estimates of the parameters (b) $\gamma(0)$, (c) $\rho(1)$, (d) α, (e) σ^2, (f) $-\tau = -A\lambda$
The broken linear trend (red line) crosses the x-axis in the year 2026, which is a very, very weak indication of a possible AMOC collapse in that year.

3. IMPROVED MONITORING OF EARLY-WARNING SIGNS

Trusting that models of the type discussed in the previous section contain a kernel of truth and increases in variance and autocorrelation are indeed possible early-warning signs of an imminent transition in a dynamical system, I will try in this section to improve the classical rolling-window technique, which typically detects changes only with a considerable delay, in particular of course when the window size is 50 or even more years.

3.1 TREND ESTIMATION

In the case of the first moment, beating the rolling window is a trivial exercise. An obvious shortcoming of using a moving average for the estimation of a trend are the missing values at each end of the observation period. Clearly, it makes a huge difference whether the extrapolation is started at the end of the observation period or 50 years earlier. A small error in the slope is irrelevant for a forecast horizon of a few months but will certainly invalidate any long-term predictions. Fortunately, missing values are no longer a problem when the trend is estimated by a global nonparametric smoothing technique like the Hodrick-Prescott (HP) filter, which strikes a balance between goodness of fit and smoothness by minimizing

$$\sum_{t=1}^{n}(X_t - F_t)^2 + \Lambda \sum_{t=3}^{n}((F_t - F_{t-1}) - (F_{t-1} - F_{t-2}))^2. \tag{9}$$

The first term vanishes if the trend estimate F_t is equal to X_t and the second term vanishes if F_t grows linearly, hence there is a trade-off between goodness of fit and smoothness. The larger the parameter Λ, the more will deviations from linearity be penalized. For the calculation of the HP trend F_t, I used the function hpfilter of the R package mFilter.

Figure 2 shows HP-trend estimates for the global mean SST (GLOBAL), the mean temperature of the subpolar gyre (SUBPOLAR), and several AMOC proxies. The red trend lines were obtained with $\Lambda = 2.5 \cdot 10^9$ and the more volatile blue trend lines with $\Lambda = 2.5 \cdot 10^7$. In the following, I will refer to the former trend estimates as slow trend and to the latter as fast trend. The slow trend (red line) of GLOBAL (see 2.a) shows a substantial increase due to global warming after a relatively stable period. This is not the case for SUBPOLAR. But then again, the

fast trend (blue line) of the latter time series exhibits a distinct low-frequency oscillation, which is called the Atlantic Multidecadal Oscillation (AMO). Clearly, this striking pattern has to be taken into account when temperature trends (or cotrends) are investigated (see, e.g., Estrada et al., 2017; Estrada and Perron, 2019). The most obvious way to deal with the AMO properly is to remove it. But that is easier said than done because each cycle has a different period, phase, amplitude, and non-sinusoidal shape. In a frequency-domain analysis, Mangat and Reschenhofer (2020) solved the problem just by omitting selected Fourier frequencies. Among the AMOC proxies examined by Boers (2021), there is one for which AMO variability has been removed. This is the only reason, why I included the fast trend. Subtracting this trend also removes the AMO. However, the AMO is rather a fluctuation about the trend than a part of the trend. When the AMO is not removed it contributes significantly to the rising variance because the amplitudes of the AMO cycles are obviously increasing over time (see Figure 2.b). In the next subsection, a criterion will be introduced which allows to compare the quality of different trend estimates. According to this criterion, the fast trend is indeed worse than the slow trend.

The three AMOC proxies shown in Figures 2.c,d,e are defined as SUBPOLAR minus j=1,2,3 times GLOBAL. Ditlevsen & Ditlevsen (2023) justified the factors j=2 and j=3 with polar amplification (see Holland and Bitz, 2003). Subtracting a time series with an upward trend from a time series with no obvious trend produces a time series with a downward trend. This transformation can help to make it clear that the temperature of the subpolar gyre defies global warming. However, as far as only the trend is concerned it might suffice to subtract just the slow trend of GLOBAL from SUBPOLAR (see Figures 2.f,g,h). Why would we want to pollute our data with global noise? And if our only goal is to estimate the variance and the autocorrelation, there is definitely no reason to overshoot (e.g., by selecting j=3). Trend removal is a necessary first step before we can calculate second moments. Why would we care to subtract a trend from a different time series when we later have to remove the combined trend anyway?

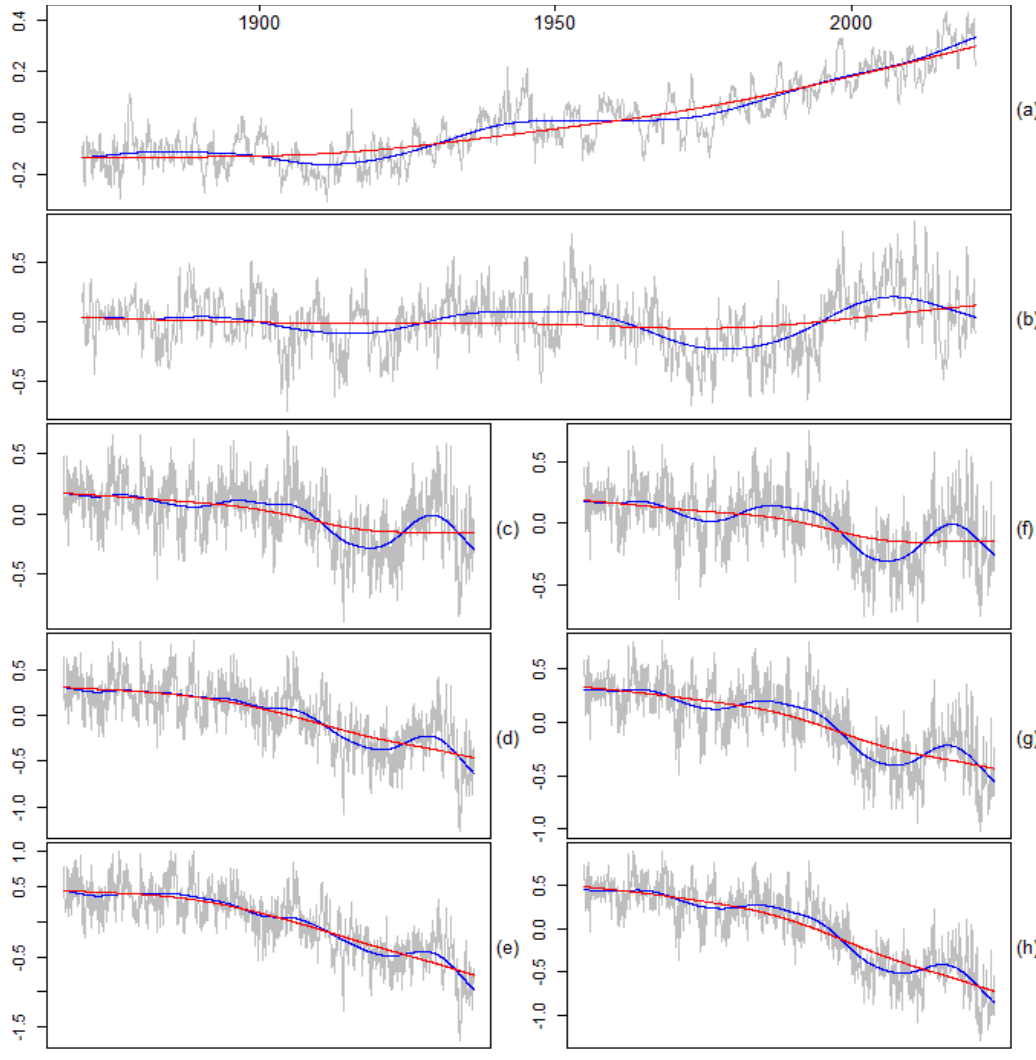

Figure 2: Trend estimates obtained by applying the HP-filter with $\Lambda = 2.5 \cdot 10^9$ (red lines) and $\Lambda = 2.5 \cdot 10^7$ (blue lines) to (a) the global mean SST, (b) the mean temperature of the subpolar gyre, (c)-(e) AMOC proxies defined as the mean temperature of the subpolar gyre minus j=1,2,3 times the global mean SST, (f)-(h) AMOC proxies defined as the mean temperature of the subpolar gyre minus j=1,2,3 times the slow trend (red line) of the global mean SST

Replacing just the trend estimate of Ditlevsen & Ditlevsen (2023), which is obtained by fitting a linear trend line within each estimation window, by the slow trend (red line in Figure 3.a) and leaving everything else unchanged has almost no effect on the estimate $\hat{t}_c$ of the tipping time (compare the green line and the red line in Figure 3.d). However, when the fast trend (blue line in Figure 3.a) is

used, the estimate $\hat{t}_c$ moves well into the next century (blue line in Figure 3.d). Regardless of which of the time series SUBPOLAR minus j=0,1,2,3 times GLOBAL or SUBPOLAR minus j=1,2,3 times the slow trend of GLOBAL is used, the estimate $\hat{t}_c$ is always in the next century when the fast trend is used and otherwise always in the first half of the current century.

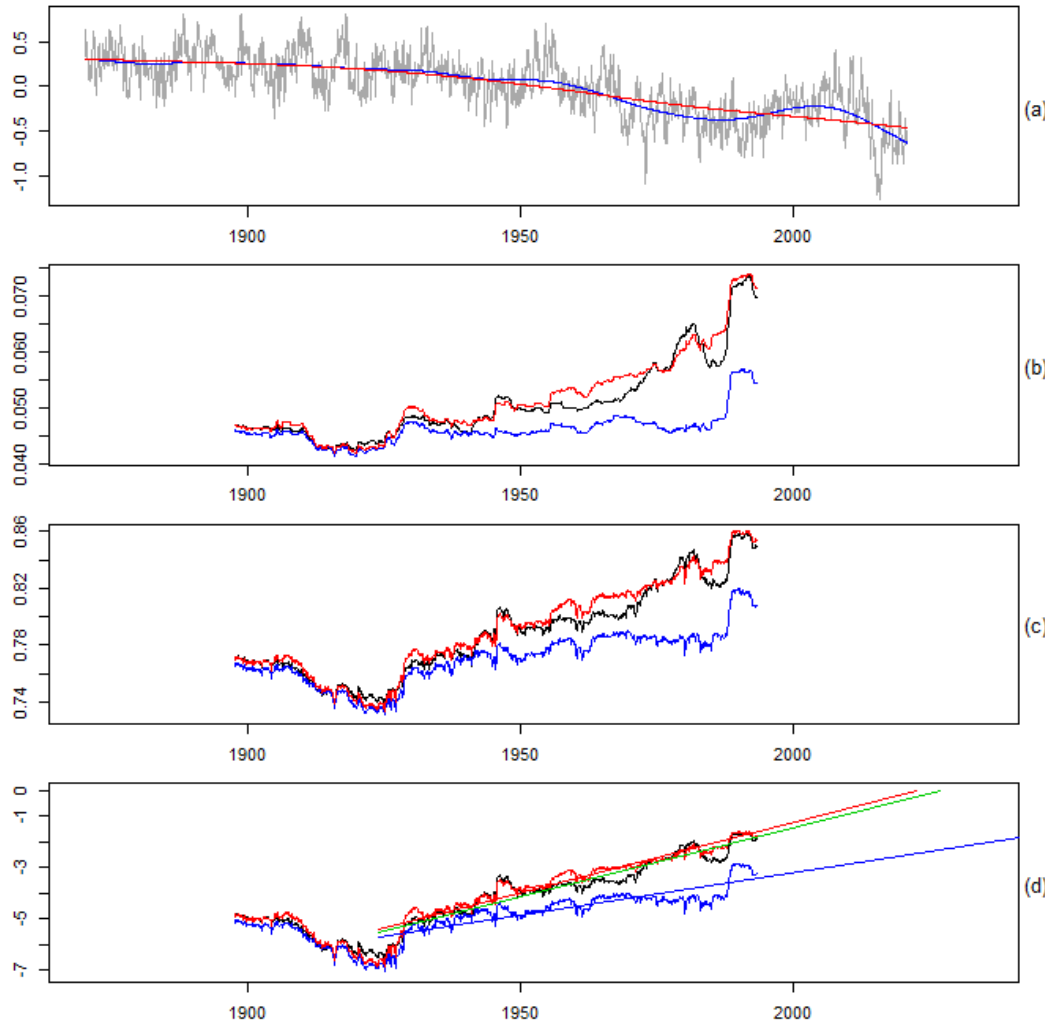

Figure 3: (a) AMOC proxy defined as the mean temperature of the subpolar gyre minus two times the global mean SST with two HP-trend estimates
(b)-(f) Rolling-window estimates of the parameters (b) $\gamma(0)$, (c) $\rho(1)$, (d) $\tau = A\lambda$
Differences are due to different methods for trend estimation: (i) linear trend within each window (green), (ii) HP-filter with $\Lambda = 2.5 \cdot 10^9$ (red), (iii) HP-filter with $\Lambda = 2.5 \cdot 10^7$ (blue)

3.2 ESTIMATION OF VARIANCE AND COVARIANCE

Little is gained when trend estimates are available for the whole observation period from 1870 to 2020 but estimates of the variance $\gamma(0)$ and the autocorrelation $\rho(1)$, which are used as early-warning signs, are still obtained from rolling windows and are therefore only available from July 1897 to June 1993. However, given the trend residuals $D_1, \ldots, D_n$ for the whole observation period, it might be sufficient for the purpose of monitoring to plot the cumulative sums

$$\frac{1}{n}\sum_{t=1}^{s} D_t^2 \, , s = 1, \ldots, n, \tag{10}$$

and

$$\frac{1}{n}\sum_{t=2}^{s} D_{t-1} D_t \, , s = 1, \ldots, n. \tag{11}$$

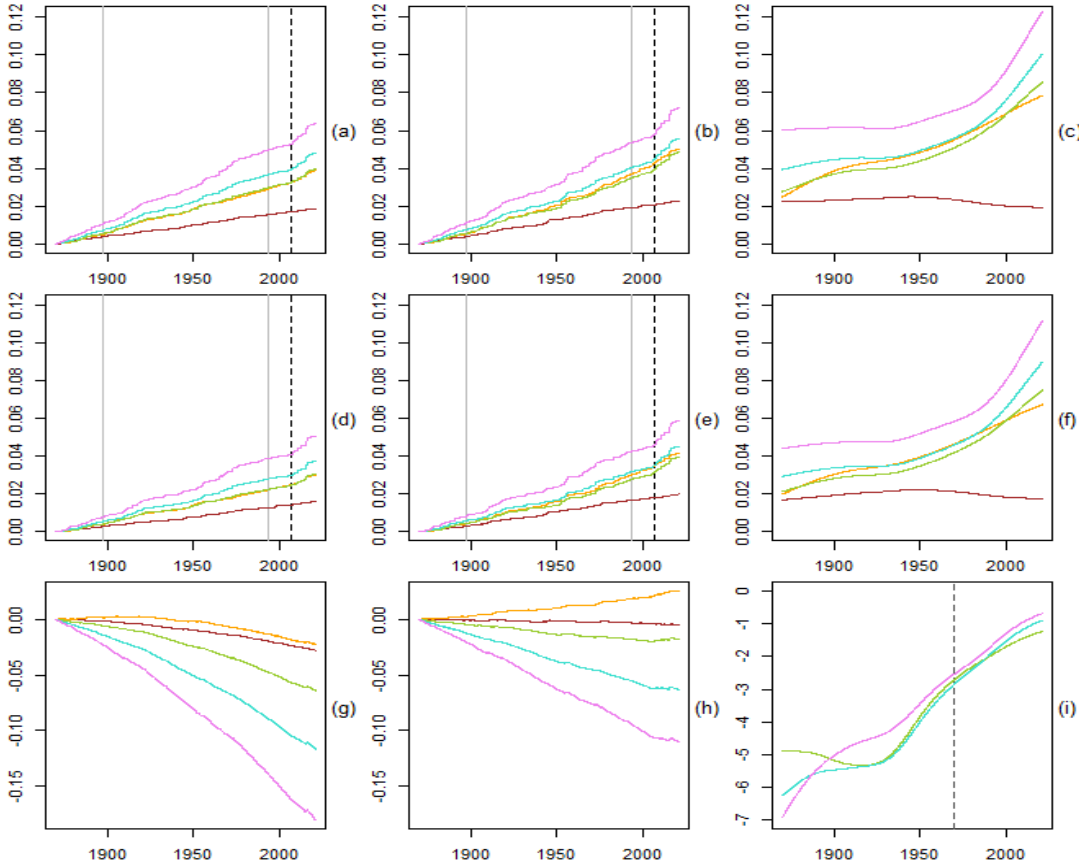

Figure 4: Searching for changes in the second moments of GLOBAL (brown line inflated with factor 5) and SUBPOLAR – j=0,1,2,3·GLOBAL (orange, yellow green, turquoise, violet)

(a) Cumulative sum of squared deviations Z_t^2 from fast trend, (d) Cumulative sum of $Z_{t-1}Z_t$
(b) Cumulative sum of squared deviations V_t^2 from slow trend, (e) Cumulative sum of $V_{t-1}V_t$
(c) Slow HP-trend of V_t^2, (f) Slow HP-trend of $V_{t-1}V_t$, (i) Estimates of τ obtained from (c) and (f)
(g), (h) Cumulative deviations of $2\left(S_Z^0(j) - S_Z^1(j)\right)$ and $2(S_V^0(j) - S_V^1(j))$ from benchmark $S(j)$
The vertical gray lines indicate the maximum range of the rolling-window approach.
Black dashed line: December 2006, dark gray dashed line: December 1969

Any deviation from linearity is a clear indication of a change in the variance $\gamma(0)$ and the covariance $\gamma(1)$, respectively. Figures 4.a,b,d,e show significant deviations after 2006 indicating increases in both variance and covariance. Since ratios of $V_{t-1}V_t$ and V_t^2 are fundamentally unstable, the straightforward production of an analogous figure for the autocorrelation is pointless unless a special trick is used, which will be introduced in Subsection 3.4. At the moment, smoothing is the only option. Estimates of $\rho(1)$ can be obtained by dividing the slow HP-trend of $V_{t-1}V_t$ (see Figure 4.f) by the slow HP-trend of V_t^2 (see Figure 4.c). These estimates can then be used to calculate estimates of τ via (7). Linear extrapolation of the values after 1969 (see Figure 4.i) yields the years 2059, 2039, and 2035 as possible transition times for the proxies SUBPOLAR – j=1,2,3·GLOBAL. Figures 4.g,h, which justify the use of only the slow trend for prediction, will be explained in the next subsection.

3.3 COMPARISON OF DIFFERENT TREND ESTIMATES

For a process (X_t) that is stationary around a slowly time-varying mean (μ_t), we have

$$\begin{aligned} E(X_t^2 - X_t X_{t+k}) &= E(X_t^2 - \mu_t^2) - E(X_t X_{t+k} - \mu_t^2) \\ &= (EX_t^2 - \mu_t^2) - (EX_t X_{t+k} - \mu_t \mu_{t+k}) - \mu_t(\mu_{t+k} - \mu_t) \\ &= \gamma(0) - \gamma(k) - \mu_t(\mu_{t+k} - \mu_t) \end{aligned} \quad (12)$$

and

$$\begin{aligned} E(X_t^2 - X_t X_{t+k}) + E(X_t^2 - X_t X_{t-k}) &= 2\sigma_y^2 - 2\gamma(k) - \mu_t(\mu_{t+k} - \mu_t) - \mu_t(\mu_{t-k} - \mu_t) \\ &\approx 2\gamma(0) - 2\gamma(k), \end{aligned} \quad (13)$$

hence the constancy of the variance $\gamma(0)$ and the kth-order autocovariance $\gamma(k)$ can be checked without worrying about the unknown mean just by plotting the cumulative sums

$$S(j) = \frac{1}{n-2k} \sum_{t=k+1}^{j} (2X_t^2 - X_t X_{t+k} - X_t X_{t-k}), j = k+1, \ldots, n-k, \quad (14)$$

against $j = k+1, \ldots, n-k$. Any significant deviation from linearity can safely be interpreted as an indication of nonconstancy. In contrast, the results obtained by carrying out a mean correction and plotting the cumulative sums

$$S_W^0(j) = \frac{1}{n} \sum_{t=1}^{j} W_t^2 = \frac{1}{n} \sum_{t=1}^{j} (X_t - \hat{\mu}_t)^2, j = 1, \ldots, n, \quad (15)$$

and

$$S_W^k(j) = \frac{1}{n-k} \sum_{t=k+1}^{j} W_t W_{t-k} = \frac{1}{n-k} \sum_{t=k+1}^{j} (X_t - \hat{\mu}_t)(X_{t-k} - \hat{\mu}_{t-k}), j = k+1, \ldots, n, \quad (16)$$

separately depend critically on the quality of the estimator $\hat{\mu}_t$. The deviations of the cumulative sum $2(S_W^0(j) - S_W^k(j))$ from the cumulative sum $S(j)$ can therefore be used to assess the quality of $\hat{\mu}_t$. A comparison of Figure 4.g with Figure 4.h suggests that the slow trend outperforms the fast trend. Of course, the assumption used here, namely local linearity of the trend, i.e., $\mu_{t+k} - \mu_t \approx -(\mu_{t-k} - \mu_t)$, is completely unproblematic, particularly in the case $k = 1$.

3.4 ESTIMATION OF AUTOCORRELATION

Reschenhofer (2019) proposed to use suitably transformed ratios of successive observations for the estimation of the first-order autocorrelation $\rho(1)$. The transformation serves to ensure the existence of all moments. It is given by

$$R_t = sign(X_{t-1}X_t)\frac{\min(|X_{t-1}|,|X_t|)}{\max(|X_{t-1}|,|X_t|)} \tag{17}$$

(for asymptotic properties of statistics of this type see Reschenhofer, 2017b). Since the sample mean $\bar{R}$ is a severely biased estimator for $\rho(1)$, Reschenhofer (2019) introduced the improved estimator

$$\hat{\rho}_1 = h^{-1}(\bar{R}), \tag{18}$$

where

$$h(\rho) = \rho + \frac{\sqrt{1-\rho^2}}{\pi}\log\left(\frac{1-\rho}{1+\rho}\right), \tag{19}$$

as well as the more comfortable approximation

$$\hat{\rho}_2 = -1 + 2\Phi_{0.295}(\bar{R}), \tag{20}$$

where Φ_σ denotes the cumulative distribution function of a normal distribution with mean 0 and standard deviation σ. A further simplification is possible if $|\rho|$ is small (see Reschenhofer, 2017a). For $|\rho| < 0.2$, the approximation

$$\hat{\rho}_3 = \frac{\pi}{\pi-2}\bar{R} \tag{21}$$

is usually accurate enough. A decisive advantage of (21) is that

$$\hat{\rho}_3 = \frac{1}{n-1}\sum_{t=2}^{n}\frac{\pi}{\pi-2}R_t, \tag{22}$$

which allows the almost instantaneous detection of a change in $\rho(1)$ just by plotting (22) cumulatively against time.

In contrast to Reschenhofer (2017a), who dealt with financial data, it is certainly not justifiable in the case of an AMOC proxy to assume that its autocorrelation is small. A way to get rid of the high autocorrelation would be to

intentionally pollute the data X_t with white noise ε_t . If the variance of ε_t is equal to the variance $\gamma(0)$ of X_t, it follows from

$$E(X_t + 3\varepsilon_t)(X_{t-1} + 3\varepsilon_{t-1}) = \gamma(1),\ E(X_t + 3\varepsilon_t)^2 = 10\,\gamma(0), \tag{23}$$

that the first-order autocorrelation of $X_t + 3\varepsilon_t$ is 10 times smaller than $\rho(1)$. The estimate obtained from the polluted data must therefore be multiplied by 10. To eliminate the dependence on a single realization of white noise it is advisable to generate a large number of realizations and calculate the mean over all estimates. However, since this solution requires the reliable estimation of the time-varying variance (for example, by applying the HP-filter to the squared trend residuals), it would nullify the key advantage of the statistic (17), namely its independence from the variance. So it might even be better to stick with the estimator (21) and accept its bias, the more so as it is possible to get helpful benchmarks with simulation (using a simple autoregressive model of order 1). In Figure 5, the statistic (17) times $\pi/(\pi - 2)$ is plotted cumulatively for the AMOC proxies SUBPOLAR – j=1,2,3·GLOBAL together with comparative lines representing the autocorrelation levels $\rho = 0.8$, $\rho = 0.85$, and $\rho = 0.9$. Instead of a steady increase in the autocorrelation there are three stable regimes of approximately constant autocorrelation. First it is about 0.8, then about 0.85, and in the last few years slightly above 0.9. It is impossible to read from this figure how long the third regime will last and what the next value will be. Remarkably, in this case there is complete agreement between the different proxies.

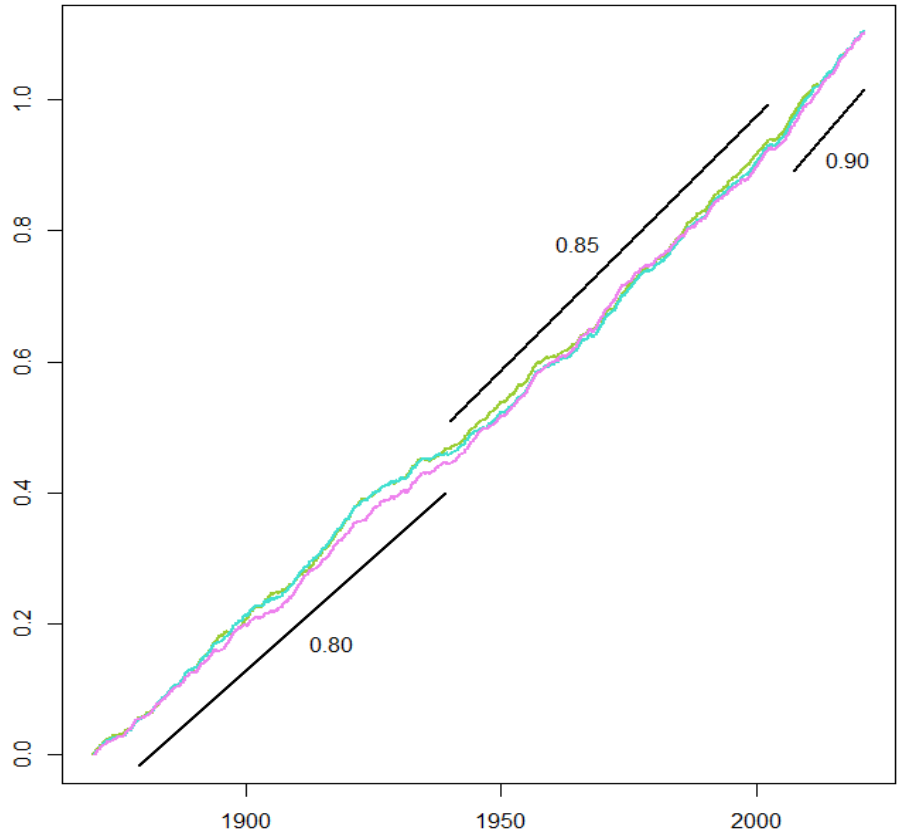

Figure 5: Monitoring the increase in first-order autocorrelation (from 0.8 to slightly above 0.9) with cumulative statistics based on ratios of successive observations of the AMOC proxies subpolar gyre minus 1 (yellow green), 2 (turquoise), and 3 (violet) times the global mean sea-surface temperature

4. DISCUSSION

Some climate models concede the possibility that the AMOC could transition from the present strong mode to a weak mode (see Boers, 2021; Ditlevsen and Ditlevsen, 2023), which would have serious consequences for the global climate. Unfortunately, there are no direct measurements of the AMOC before 2004. When certain studies require longer time series, they must resort to proxies which are based on measurements of sea-surface temperature or salinity (Rahmstorf et al., 2015; Caesar et al., 2018; Jackson and Wood, 2020; Boers, 2021). Using a new AMOC proxy and certain early-warning signs like an increase in variance and autocorrelation, Ditlevsen & Ditlevsen (2023) estimated that the AMOC could

collapse by the middle of the century. However, after a careful review of their study, I think that it is not possible at this time to say with any certainty if and when a collapse of the AMOC will occur. There are simply too many uncertainties concerning the validity of the underlying model, the choice of the AMOC proxy, the plausibility of certain assumptions, the adequacy of certain approximations, the efficiency of the employed estimation methods, the extent of data snooping for the determination of the size of the rolling window and the break point in a broken linear trend, etc. Playing around a bit with the tuning parameters, you can just get any answer from "the transition has already happened long ago" to "it will never happen".

Of course, there is plenty of room for improvement. For example, the sea region that is used for the construction of the AMOC proxy could be defined in a more objective way (Reschenhofer, 2024a) or the naive seasonal-adjustment method of just subtracting the monthly means could be replaced by a more sophisticated method that is appropriate also in case of a time-changing seasonal pattern (Reschenhofer, 2024b). But the introduction of any further amendment option would inevitably increase the complexity of the forecasting procedure and thereby possibly also its volatility. It may therefore make more sense to stop with the forecast attempts and just focus on the monitoring of the early-warning signs. Several improvements have been introduced in this study, which allow the monitoring of the early-warning signs without any delay caused by a long estimation window that spans over 50 years or more. One result obtained with these new methods is of particular interest. It suggests that the increase in the autocorrelation is due to only two structural breaks rather than a steady change (see Figure 5) and can therefore not be used for extrapolation. Of course, the findings of this study give no cause to sound the all-clear. After all, the low reliability of the prediction of a near tipping point does not imply that the opposite is true.

References

[1] N. Boers, Observation-based early-warning signs for a collapse of the Atlantic Meridional Overturning Circulation. Nat. Climate Change. 11 (2021) 680–688. https://doi.org/10.1038/s41558-021-01097-4.

[2] L. Caesar, S. Rahmstorf, A. Robinson, G. Feulner, V. Saba, Observed fingerprint of a weakening Atlantic Ocean overturning circulation. Nature. 556 (2018) 191–196. https://doi.org/10.1038/s41586-018-0006-5.

[3] P. Ditlevsen, S. Ditlevsen, Warning of a forthcoming collapse of the Atlantic meridional overturning circulation. Nat. Comm. 14 (2023) 4254. https://doi.org/10.1038/s41467-023-39810-w.

[4] F. Estrada, L.F. Martins, P. Perron, Characterizing and attributing the warming trend in sea and land surface temperatures. Atmósfera. 30 (2017) 163–187. https://doi.org/10.20937/atm.2017.30.02.06.

[5] F. Estrada, P. Perron, Breaks, trends and the attribution of climate change: A time-series analysis. Economía. 42 (2019) 1–31. https://doi.org/10.18800/economia.201901.001.

[6] IPCC, Summary for Policymakers. In: IPCC Special Report on the Ocean and Cryosphere in a Changing Climate [H.-O. Portner, D.C. Roberts, V. Masson-Delmotte, P. Zhai, M. Tignor, E. Poloczanska, K. Mintenbeck, A. Alegría, M. Nicolai, A. Okem, J. Petzold, B. Rama, N.M. Weyer (eds.)]. Cambridge University Press, Cambridge, UK and New York, NY, USA, (2019) 3-35. https://doi.org/10.1017/9781009157964.001.

[7] M.M. Holland, C.M. Bitz, Polar amplification of climate change in coupled models. Climate Dyn. 21 (2003) 221–232. https://doi.org/10.1007/s00382-003-0332-6.

[8] L.C. Jackson, R.A. Wood, Fingerprints for early detection of changes in the AMOC. J. Climate 33 (2020) 7027–7044. https://doi.org/10.1175/jcli-d-20-0034.1.

[9] M. Latif, E. Roeckner, M. Botzet, M. Esch, H. Haak, S. Hagemann, J. Jungclaus, S. Legutke, S. Marsland, U. Mikolajewicz, J. Mitchell, Reconstructing, monitoring, and predicting multidecadal-scale changes in the North Atlantic thermohaline circulation with sea surface temperature. J. Climate. 17 (2004) 1605-1614. https://doi.org/10.1175/1520-0442(2004)017<1605:RMAPMC>2.0.CO;2.

[10] M.K. Mangat E. Reschenhofer (2020) Frequency-domain evidence for climate change. Econometrics. 8 (2020) 28. https://doi.org/10.3390/econometrics8030028.

[11] S. Rahmstorf, J.E. Box, G.Feulner, M.E. Mann, A.Robinson, S.Rutherford, E.J. Schaffernicht, Exceptional twentieth-century slowdown in Atlantic Ocean overturning circulation. Nat. Climate Change. 5 (2015) 475–480. https://doi.org/10.1038/nclimate2554.

[12] R Core Team, R: A language and environment for statistical computing. R Foundation for Statistical Computing, Vienna, Austria (2022). https://www.R-project.org.

[13] N.A. Rayner, D.E. Parker, E.B. Horton, C.K. Folland, L.V. Alexander, D.P. Rowell, E.C. Kent, A. Kaplan, Global analyses of sea surface temperature, sea ice, and night marine air

temperature since the late nineteenth century. J. Geophys. Res. 108 (2003) 4407. https://doi.org/10.1029/2002jd002670.

[14] E. Reschenhofer, Using ratios of successive returns for the estimation of serial correlation in return series. Noble Int. J. Econ. Financial Res. 02/09 (2017a) 125-130.

[15] E. Reschenhofer, Examining the properties of a simple estimator based on transformed Cauchy variables. J. Stat.: Adv. Theory Appl. 18 (2017b) 45-54. https://doi.org/10.18642/jsata_7100121869.

[16] E. Reschenhofer, Heteroscedasticity-robust estimation of autocorrelation. Comm. Stat. – Simul. Comp. 48/4 (2019) 1251–1263. https://doi.org/10.1080/03610918.2017.1408826.

[17] E. Reschenhofer, Reassessment of the subpolar gyre's predictive power. Working paper. (2024a).

[18] E. Reschenhofer, Coping with seasonal effects of global warming in the estimation of second moments. Int. J. Stat. Appl. 14 (2024b) 1-6.